PCP
PLANT & CELL PHYSIOLOGY

Dominant-Negative KAI2d Paralogs Putatively Attenuate Strigolactone Responses in Root Parasitic Plants

Alexandra R.F. White[1], Annalise Kane[1], Satoshi Ogawa[1,2,3], Ken Shirasu[2] and David C. Nelson[1,*]

[1]Department of Botany and Plant Sciences, University of California, 3401 Watkins Drive, Riverside, CA 92521, USA
[2]Plant Immunity Research Group, RIKEN Center for Sustainable Resource Science, 1-7-22 Suehiro-cho, Tsurumi-ku, Yokohama 230-0045, Japan
[3]Present address: Institute for Chemical Research, Kyoto University, Uji, 611-0011 Japan.

*Corresponding author: E-mail, david.nelson@ucr.edu

(Received 5 April 2024; Accepted 12 September 2024)

Many root parasitic plants in the Orobanchaceae use host-derived strigolactones (SLs) as germination cues. This adaptation facilitates attachment to a host and is particularly important for the success of obligate parasitic weeds that cause substantial crop losses globally. Parasite seeds sense SLs through 'divergent' KARRIKIN INSENSITIVE2 (KAI2d)/HYPOSENSITIVE TO LIGHT α/β-hydrolases that have undergone substantial duplication and diversification in Orobanchaceae genomes. After germination, chemotropic growth of parasite roots toward a SL source also occurs in some species. We investigated which of the seven *KAI2d* genes found in a facultative hemiparasite, *Phtheirospermum japonicum*, may enable chemotropic responses to SLs. To do so, we developed a triple mutant *Nbd14a,b kai2i* line of *Nicotiana benthamiana* in which SL-induced degradation of SUPPRESSOR OF MORE AXILLARY GROWTH2 (MAX2) 1 (SMAX1), an immediate downstream target of KAI2 signaling, is disrupted. In combination with a transiently expressed, ratiometric reporter of SMAX1 protein abundance, this mutant forms a system for the functional analysis of parasite KAI2d proteins in a plant cellular context. Using this system, we unexpectedly found three PjKAI2d proteins that do not trigger SMAX1 degradation in the presence of SLs. Instead, these PjKAI2d proteins inhibit the perception of low SL concentrations by SL-responsive PjKAI2d in a dominant-negative manner that depends upon an active catalytic triad. Similar dominant-negative *KAI2d* paralogs were identified in an obligate hemiparasitic weed, *Striga hermonthica*. These proteins suggest a mechanism for attenuating SL signaling in parasites, which might be used to enhance the perception of shallow SL gradients during root growth toward a host or to restrict germination responses to specific SLs.

Keywords: Chemotropism • Feedback inhibition • *Nicotiana benthamiana* • Parasitism • Signaling

Introduction

Root parasitic plants in the Orobanchaceae have adapted to sense chemical signals exuded into soil from plant roots (Bouwmeester et al. 2021). Typically, these signals are strigolactones (SLs), a family of carotenoid-derived compounds that play roles in hormonal regulation of plant development and recruitment of beneficial symbiotic associations with microbes (Waters et al. 2017, Kee et al. 2023, Clark et al. 2024). Many of the obligate parasites in the Orobanchaceae use SLs as a cue for germination, which makes it more likely for a nascent seedling to find and attach to a potential host before it exhausts its supply of nutrients (Cook et al. 1966, Mutuku et al. 2021, Ogawa and Shirasu 2022). Chemicals exuded from host roots are also used by parasitic seedlings to orient the direction of radicle elongation (Williams 1961, Whitney and Carsten 1981, Krupp et al. 2021). Chemotropic growth toward SLs has been observed in an obligate hemiparasite, *Striga hermonthica*, which requires a host to complete its life cycle, as well as in a facultative hemiparasite, *Phtheirospermum japonicum*, which can grow independent of a host or engage in parasitism opportunistically (Ogawa et al. 2022).

Host-derived SLs are perceived by the seed of root parasites through a mechanism that has been adapted from karrikin (KAR) signaling (Conn et al. 2015, Toh et al. 2015, Tsuchiya et al. 2015, Nelson 2021). KARs are butenolide compounds found in smoke that stimulate germination of many plants in the soil seed bank after fire (Flematti et al. 2004, Nelson et al. 2012). KAR perception is mediated by an α/β-hydrolase, KARRIKIN INSENSITIVE2 (KAI2), also known as HYPOSENSITIVE TO LIGHT (HTL) (Sun and Ni 2011, Waters et al. 2012). Activation of KAI2 stimulates interactions with an F-box protein, MORE AXILLARY GROWTH2 (MAX2)/DWARF3 (D3), and putative transcriptional co-repressor proteins, SUPPRESSOR OF MAX2 1 (SMAX1) and SMAX1-LIKE2 (SMXL2) (Stanga et al. 2013, Wang et al. 2020, Zheng et al. 2020, Khosla et al. 2020a).

Plant Cell Physiol. 65(12): 1969–1982 (2024) doi:https://doi.org/10.1093/pcp/pcae106, Advance Access publication on 13 September 2024, available online at https://academic.oup.com/pcp

MAX2 acts as an adapter that confers substrate specificity to an SCF-type (Skp1, Cullin, F-box) E3 ubiquitin ligase complex (Stirnberg et al. 2007). KAI2–SCF^{MAX2} polyubiquitinates SMAX1 and SMXL2, marking them for rapid degradation by the 26S proteasome (Wang et al. 2020, Zheng et al. 2020, Khosla et al. 2020a). Degradation of SMAX1 and SMXL2 then initiates various downstream growth responses including seed germination (Stanga et al. 2013, 2016, Bunsick et al. 2022, Waters and Nelson 2023). A very similar mechanism is used by spermatophytes in the perception of endogenous SL hormones. A paralog of KAI2, DWARF14 (D14)/DECREASED APICAL DOMINANCE2 (DAD2), is an SL receptor that works with SCF^{MAX2} to target several SMAX1-LIKE (SMXL) proteins for degradation (Hamiaux et al. 2012, Yao et al. 2016, Blázquez et al. 2020). In *Arabidopsis thaliana*, SMXL6, SMXL7 and SMXL8 (orthologs of DWARF53 in *Oryza sativa*) are the primary targets of D14–SCF^{MAX2}, but SMAX1 and SMXL2 can also be targeted when SL is applied or putatively increased during osmotic stress (Jiang et al. 2013, Zhou et al. 2013, Soundappan et al. 2015, Wang et al. 2015a, 2020, Li et al. 2022).

Mounting evidence suggests that although KAI2 can mediate responses to KARs (or, more likely, a KAR metabolite), its usual function is the perception of an unknown endogenous signal(s) known as 'KAI2 ligand' (KL) (Conn and Nelson 2015, Waters and Nelson 2023). One to a few copies of *KAI2* are typically present in angiosperm genomes. *KAI2* paralogs have shown varied ligand preferences for KL, different KARs, (−)-germacrene D or synthetic KAI2 agonists, which suggests adaptation for perceiving different signals (Carbonnel et al. 2020, Sun et al. 2020, Martinez et al. 2022, Stirling et al. 2024). In the parasitic Orobanchaceae, *KAI2* has undergone an unusual expansion in copy number that is particularly dramatic among obligate parasites such as *Striga* spp. (Conn et al. 2015, Toh et al. 2015, Yoshida et al. 2019, Nelson 2021). The majority of the new *KAI2* paralogs fall into a rapidly evolving, 'divergent' clade, *KAI2d* (Conn et al. 2015, Nelson 2021). KAI2d proteins from the root parasitic species *S. hermonthica, Phelipanche aegyptiaca*, *P. ramosa, Orobanche minor* and *O. cumana* have been demonstrated to perceive SLs (Conn et al. 2015, Toh et al. 2015, Tsuchiya et al. 2015, Yao et al. 2017, de Saint Germain et al. 2021, Wang et al. 2021, Larose et al. 2022, Takei et al. 2023). In addition, a KAI2d protein from *P. ramosa* responds to isothiocyanates (de Saint Germain et al. 2021). Therefore, the *KAI2d* clade arose from gene duplication and underwent neofunctionalization that changed the ligand preferences of KAI2 proteins, similar to the evolution of D14. The transition to SL perception in KAI2 proteins can evolve through as few as three mutations in the ligand-binding pocket (Arellano-Saab et al. 2021). It is also remarkable that some KAI2d proteins, such as *S. hermonthica* HTL7 (ShHTL7), confer sensitivity to extraordinarily low (e.g. picomolar) concentrations of SLs although this is more a consequence of unusually high affinity for MAX2 rather than for SL (Toh et al. 2015, Tsuchiya et al. 2015, Wang et al. 2021).

Why parasite genomes contain so many *KAI2d* paralogs remains an unresolved question. One potential explanation is that individual KAI2d proteins may specialize in perception of different SLs, of which more than 30 have been identified (Conn et al. 2015, Bouwmeester et al. 2021, Nelson 2021). This would putatively enable a parasite to respond to a specific chemical fingerprint that corresponds to a compatible host. Indeed, variable affinities for different SLs have been observed in the germination responses of some parasites as well as among KAI2d proteins in vitro and in vivo (Fernández-Aparicio et al. 2011, Toh et al. 2015, Tsuchiya et al. 2015, Wang et al. 2021). Broadening the range of SLs that can be perceived, putatively through *KAI2d* evolution, can lead to rapid expansions in the host range, as illustrated by the recent emergence of a race of sunflower broomrape, *O. cumana*, that can also attack tomato (Dor et al. 2020). Thus, the antagonistic coevolution of hosts and plant parasites could drive diversification of SL biosynthesis and SL detection mechanisms, respectively.

A second idea is that *KAI2d* simply may be prone to gene duplication. The observation of localized duplication of *KAI2d* genes in different parasite genomes suggests that they have arisen through mechanisms such as unequal crossing over, which is facilitated by repetitive genetic sequences (Yoshida et al. 2019, Xu et al. 2022). It is possible that very few *KAI2d* genes in a genome are involved in host perception and that most *KAI2d* copies either are pseudogenes or have little or no adaptive value. Notably, chemical stimulation of ShHTL7 alone is sufficient to trigger germination of *S. hermonthica*, implying that other KAI2d proteins may be unnecessary in that species, at least in seed (Uraguchi et al. 2018).

A third possibility, which has not yet been tested, is that some KAI2d proteins may have antagonistic effects on parasite germination (Nelson 2021). This idea arose from the observation that closely related root parasites, such as *S. hermonthica* and *Striga gesnerioides* or species within the *Orobanche*/*Phelipanche* genera, can show quite different responses to various SLs or host exudates during germination despite having large and highly similar sets of *KAI2d* genes (Fernández-Aparicio et al. 2009, 2011, Nomura et al. 2013, Tsuchiya et al. 2015). Even intraspecific differences in germination responses to SLs have been observed for *P. ramosa* and *O. cumana* (Dor et al. 2020, Huet et al. 2020). For obligate parasites, many of which are specialists with a restricted host range, positive germination responses to SLs made by a compatible host combined with inhibitory responses to SLs made by a non-compatible host would have obvious advantages. Putatively, the most direct route for the evolution of inhibitory responses to a detrimental SL would be through the emergence of a dominant-negative (antimorphic) KAI2d protein that is activated by that SL, rather than through accruing loss-of-function mutations in all *KAI2d* paralogs that can recognize that SL (Nelson 2021). Several *KAI2d* genes from *S. hermonthica*, *O. cernua* and *O. cumana* have failed to confer SL responses to *A. thaliana* in cross-species complementation assays (Conn et al. 2015, Toh et al. 2015, Nelson 2021, Larose et al. 2022). It is unknown, however, whether any of these proteins are dominant-negative forms of KAI2d, are inactive or only seem to be inactive for other reasons (e.g.

an appropriate SL agonist was not tested, or the protein cannot form functional interactions with *Arabidopsis* SCF^{MAX2} and SMAX1/SMXL2 proteins).

Additional examples of unusual *KAI2d* have been described recently in *P. japonicum*. Under nutrient-deprived conditions, *P. japonicum* seedlings show chemotropic root growth toward artificial and biological SL sources (Ogawa et al. 2022). Putatively, this response is mediated by one or more *KAI2d* genes, of which up to seven are present in the *P. japonicum* genome, as *SMAX1* overexpression blocks chemotropism (Ogawa et al. 2022). *PjKAI2d1*, *PjKAI2d4*, *PjKAI2d4.2* and *PjKAI2d5* form a clade that has generally low expression in seedlings. *PjKAI2d2*, *PjKAI2d3* and *PjKAI2d3.2* form a sister clade that has comparably high expression in seedlings prior to infection of the host. Furthermore, *PjKAI2d2* and *PjKAI2d3.2* expression is induced by *rac*-strigol treatment or the absence of nutrients. These expression patterns suggested that the members of this clade are the most likely candidates for SL perception in *P. japonicum* seedlings. Indeed, overexpression of *PjKAI2d2* increases chemotropism of *P. japonicum* hairy roots toward *rac*-strigol (Ogawa et al. 2022). However, *Arabidopsis d14 kai2* lines carrying *PjKAI2d2*, *PjKAI2d3* and *PjKAI2d3.2* transgenes show little or no germination response to *rac*-strigol treatment (Ogawa et al. 2022). This raises the question of whether these KAI2d proteins function differently than typical SL receptors.

The options are currently limited for evaluating the function of KAI2d proteins from parasitic plants within a plant cellular context. A commonly used approach has been cross-species complementation, in which a *KAI2d* transgene from a parasite is introduced into a *kai2* or *d14 kai2* double mutant background in *A. thaliana*, which is easily transformed, and then evaluated for its ability to rescue seed germination or seedling growth phenotypes in the presence of candidate signaling molecules (Conn et al. 2015, Toh et al. 2015). This approach has identified KAI2d proteins with high sensitivity to SLs although its success as a bioassay is probably influenced by the affinity of each KAI2d for *Arabidopsis* MAX2 and SMAX1/SMXL2 proteins (Wang et al. 2021). One drawback is that it takes several months to more than a year to develop homozygous transgenic lines for phenotypic assays.

An alternative approach involves assaying SL responses in a transient expression system in plants. We previously made a set of vectors, pRATIO, for ratiometric analysis of protein abundance (Khosla et al. 2020b). In this system, the coding sequence (CDS) for a target protein of interest is fused to that of a reporter protein (e.g. the bright, red fluorescent protein mScarlet-I), a modified 'self-cleaving' 2A peptide from foot-and-mouth disease virus, and a reference reporter protein (e.g. the yellow fluorescent protein Venus). During translation, the target-reporter fusion protein is separated from the reference reporter protein due to ribosomal skipping induced by the 2A peptide. The ratio of target-reporter signal to reference reporter signal provides a convenient readout of relative target protein abundance in vivo. The system is deployed through injection of *Agrobacterium tumefaciens* cells carrying pRATIO plasmids into *N. benthamiana* leaves ('agroinfiltration') and measured through fluorescence or luminescence scanning of excised leaf disks for each reporter protein a few days later. This method has enabled monitoring of AtSMAX1 and AtSMXL7 degradation following KAR or SL treatments (Khosla et al. 2020a, 2020b, Li et al. 2022, White et al. 2022).

An extension of this approach is to measure the ability of co-expressed KAI2 or D14 receptor proteins to trigger SMAX1/SMXL reporter degradation, but it requires removal of the native *N. benthamiana* KAR or SL receptors. We previously isolated loss-of-function mutations in the two copies of *D14* in the *N. benthamiana* genome through CRISPR-Cas9 gene editing (White et al. 2022). The resulting *Nbd14a,b* mutant line shows developmental phenotypes that are consistent with SL insensitivity. In addition, degradation of AtSMXL7 ratiometric reporter protein after treatment with *rac*-GR24 (a racemic mixture of a synthetic SL analog, $GR24^{5DS}$ and its enantiomer, $GR24^{ent-5DS}$) or its enantiopure components is blocked (White et al. 2022). This genetic background makes it possible to assay the SL signaling activity of transiently co-expressed *D14* variants. However, it is not suitable for analyzing KAI2d function, as some degradation of SMAX1 and SMXL2 ratiometric reporters still occurs after $GR24^{5DS}$ treatment (Li et al. 2022). Putatively, this is because one or more of the KAI2 proteins in *N. benthamiana* can mediate responses to $GR24^{5DS}$.

We set out to examine the functions of the seven *P. japonicum KAI2d* genes. To do so, we improved the *N. benthamiana* platform to enable characterization of *P. japonicum* KAI2d proteins. In this heterologous plant-based assay, we found that PjKAI2d2, PjKAI2d3 and PjKAI2d3.2 do not activate SMAX1 degradation in response to SL perception, in contrast to PjKAI2d proteins from the low-expression clade. Instead, PjKAI2d2 and PjKAI2d3.2 antagonize SL signal transduction by other PjKAI2d proteins, potentially providing a mechanism to attenuate SL responses that might be useful for perceiving shallow chemical gradients during chemotropism.

Results

Generation of a SL-insensitive mutant in *N. benthamiana*

We identified four potentially functional *KAI2* genes and one pseudogene in the allotetraploid genome of *N. benthamiana* (assembly version 1.0.1) (Bombarely et al. 2012). Based on phylogenetic analysis, three genes are 'conserved'-type *KAI2* (*KAI2c*), members of a clade under strong purifying selection that has been associated with KL perception, while one is an 'intermediate'-type *KAI2* (*KAI2i*) from a less well-conserved group that has been associated with perception of KAR_1 or (−)-germacrene D (Conn et al. 2015, Stirling et al. 2024) (**Supplementary Fig. S1**).

With the goal of eliminating SL-induced degradation of SMAX1 in *N. benthamiana* leaves, we used CRISPR-SpCas9 to introduce mutations in the four *NbKAI2* genes in the *Nbd14a,b*

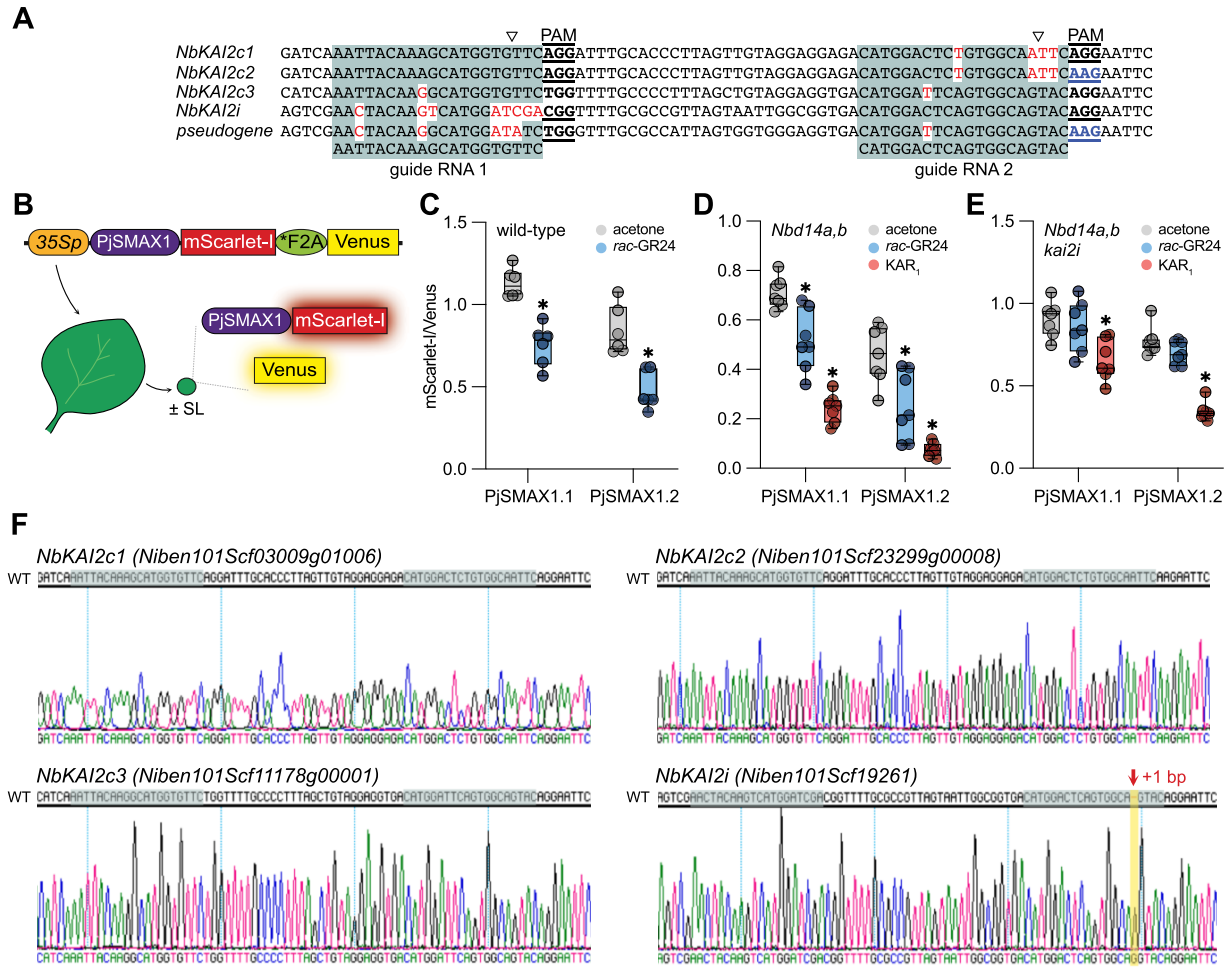

Fig. 1 Generation of an SL-insensitive *N. benthamiana* mutant. (A) Two gRNA target sites in *N. benthamiana KAI2* genes. Sequence excerpts from the second exon of the four *NbKAI2d* genes and one pseudogene are shown. Triangle, Cas9 cleavage site. Shading indicates gRNA recognition sites and matching nucleotides in *NbKAI2* genes. Protospacer adjacent motifs (PAM) 'NGG' or non-preferred 'NAG' for SpCas9 are underlined. (B) Schematic representation of the PjSMAX1 ratiometric reporter assay. pRATIO1212 construct (top, nuclear localization sequence at the N-terminal end of PjSMAX1 is not shown) is transformed into *N. benthamiana* leaves. Excised leaf disks are treated and measured for mScarlet-I and Venus fluorescence using a plate reader. (B)–(E) Ratio of PjSMAX1-mScarlet-I fluorescence to Venus fluorescence in wild-type (B), *Nbd14a,b* (C), and an SL-insensitive mutant isolated from a Nbd14a,b transgenic CRISPR-Cas9 transgenic line using gRNAs described in (A). Excised leaf disks were treated with 0.02% (v/v) acetone, 10 μM *rac*-GR24 or 10 μM KAR_1, and fluorescence was read ~16 h post-treatment. Each data point represents the average ratio of mScarlet-I to Venus fluorescence of 4–8 leaf disks from a single transformed leaf. $n = 4–7$ leaves. *$P < 0.05$, paired two-way ANOVA, comparison of treatments to acetone control with Bonferroni correction for multiple comparisons. Note that the range of mScarlet-I/Venus ratios varies between experiments due to experiment-specific optimization of gain for each fluorophore during fluorescence measurements. (F) Sanger sequence of the CRISPR-Cas9-targeted regions in the SL-insensitive mutant line identified in (E). Top sequence is reference, and bottom sequence is from the mutant. The mutant has a 1-bp insertion, which causes a frameshift, at the second gRNA site in *NbKAI2i*.

mutant background. We selected two guide RNAs (gRNAs) that could potentially target the second exon of multiple *NbKAI2* genes (**Fig. 1A**) and then transformed *Nbd14a,b* with pHEE401E, a binary plasmid that expresses maize-codon-optimized *SpCas9* from an egg cell–specific promoter and both gRNAs from U6 promoters (Wang et al. 2015b). We then used a phenotype-based screen, rather than a genotype-based screen for *NbKAI2* mutations, to identify a SL-insensitive plant. To monitor SMAX1 degradation, we introduced CDSs for the two copies of *SMAX1* that have been identified in *P. japonicum*, *PjSMAX1.1* and *PjSMAX1.2*, into the ratiometric reporter vector pRATIO1212 (Khosla et al. 2020b, Ogawa et al. 2022) (**Fig. 1B**). *PjSMAX1.1* has been suggested to be a potential pseudogene based on an atypical $(Asn)_{15}$ sequence encoded in the protein's D2 domain, which is important for MAX2-mediated degradation and coordinating interactions with TOPLESS (TPL)/TPL-RELATED transcriptional co-repressors; however, this hypothesis has not been tested (Khosla et al. 2020a, Ogawa et al. 2022). The reporter ratios

for both PjSMAX1.1 and PjSMAX1.2 declined after *rac*-GR24 treatment in wild-type *N. benthamiana* and *Nbd14a,b* leaves, suggesting that the proteins are regulated similarly (**Fig. 1C, D**). We identified a CRISPR-Cas9 transgenic line that showed no significant degradation of PjSMAX1.1 and PjSMAX1.2 ratiometric reporters in response to *rac*-GR24 treatment although it was still responsive to KAR_1 (**Fig. 1E**). This line has a one base-pair insertion mutation in *NbKAI2i* that causes a frameshift, but the other three *NbKAI2* genes are unaffected (**Fig. 1F**). Therefore, NbKAI2i is putatively responsible for the remaining *rac*-GR24 response in *Nbd14a,b*. Because we consistently observed higher reporter ratios under mock-treated conditions for PjSMAX1.1 than PjSMAX1.2, we chose to use the PjSMAX1.1 reporter as a readout of KAI2d activity in subsequent experiments.

Functional analysis of PjKAI2d proteins

We isolated a transgene-free, homozygous *Nbd14a,b kai2i* line through segregation. We then investigated the ability of the seven PjKAI2d proteins to trigger degradation of PjSMAX1.1 ratiometric reporter in *Nbd14a,b kai2i* leaves in response to SL treatment. The CDS for each gene was cloned into a binary vector, pGWB402, which drives transgene expression under the control of a *35S* promoter, and co-transformed with pRATIO1212-PjSMAX1.1. We tested the empty pGWB402 vector and pGWB402 containing the CDS of *OcKAI2d1* from the obligate holoparasite *O. cumana* as negative and positive controls, respectively (Conn et al. 2015, Larose et al. 2022).

We observed a significant decrease in the PjSMAX1.1 reporter ratio after 10 μM *rac*-GR24 treatment when *OcKAI2d1*, but not any of the *PjKAI2d*, was co-expressed in *Nbd14a,b kai2i* (**Fig. 2A**). Because *rac*-GR24 may not be an effective ligand for PjKAI2d proteins, we also tested *rac*-strigol, a racemic mixture of a naturally occurring SL and its enantiomer that attracts chemotropic growth of *P. japonicum* (Ogawa et al. 2022). In contrast to *rac*-GR24, 1 μM *rac*-strigol stimulated PjSMAX1.1 degradation in the presence of several KAI2d (**Fig. 2B**). Co-expression of *PjKAI2d1*, *PjKAI2d4* and *PjKAI2d5* caused significant reductions in the PjSMAX1.1 reporter ratio after *rac*-strigol treatment, suggesting that they are functional SL receptors. Under mock-treated conditions, the PjSMAX1.1 reporter ratio was also reduced by all three co-expressed genes relative to the empty vector control (**Fig. 2**). This may be because PjKAI2d1, PjKAI2d4 and PjKAI2d5 respond to endogenous SLs or perhaps another endogenous compound (e.g. KL), in *Nbd14a,b Nbkai2* leaves. *PjKAI2d4.2* co-expression produced a particularly low PjSMAX1.1 reporter ratio, implying that PjKAI2d4.2 has constitutive signaling activity or is even more sensitive to endogenous SLs or another endogenous compound than the other PjKAI2d proteins. In contrast, we did not observe any evidence of PjSMAX1.1 reporter degradation after *rac*-strigol treatment when *PjKAI2d2*, *PjKAI2d3* or *PjKAI2d3.2* was co-expressed (**Fig. 2B**). Furthermore, the PjSMAX1.1 reporter ratio remained similar to the empty vector control in mock-treated leaves when these genes were co-expressed (**Fig. 2**). These results suggest that

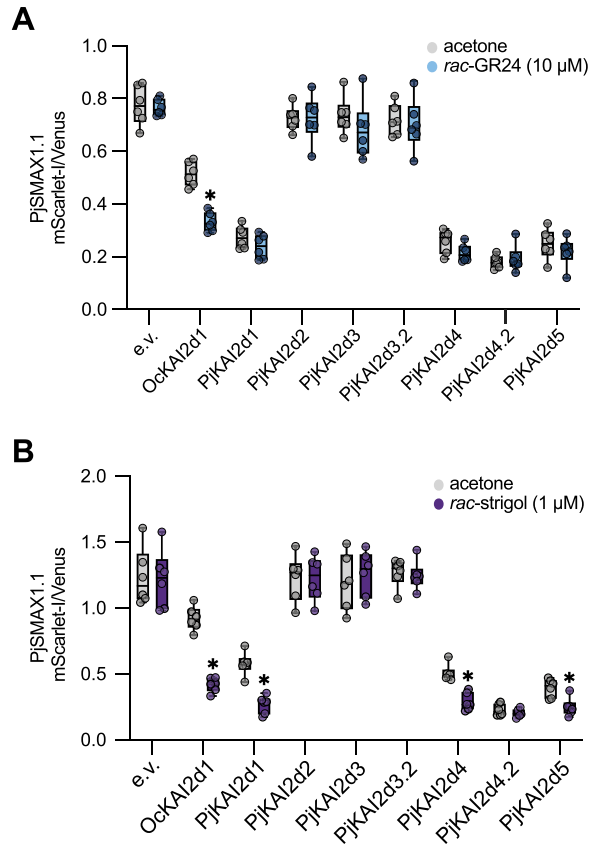

Fig. 2 Analysis of PjKAI2d activity. Analysis of PjSMAX1.1 ratiometric reporter co-transformed with pGWB402-PjKAI2d constructs in *Nbd14a,b kai2i* leaves. (A) Co-transformed leaf disks treated with 0.02% (v/v) acetone or 10 μM *rac*-GR24 treatment. (B) Co-transformed leaf disks treated with 0.01% (v/v) acetone or 1 μM *rac*-strigol treatment. $n = 6$ leaves per construct, mean ratio of 4–6 disks per leaf. *$P < 0.05$, paired two-way ANOVA, comparison of treatments to acetone control with Bonferroni correction for multiple comparisons. Box plot whiskers indicate minimum and maximum values.

PjKAI2d2, PjKAI2d3 and PjKAI2d3.2 are insensitive to SL and/or unable to transduce SL signals.

These observations conflicted with our initial hypothesis that *PjKAI2d2*, *PjKAI2d3* and *PjKAI2d3.2* are responsible for SL responses in *P. japonicum* seedlings (Ogawa et al. 2022). Therefore, we considered that PjKAI2d2, PjKAI2d3 and PjKAI2d3.2 may have atypical functions instead. Specifically, we hypothesized that these proteins may competitively inhibit PjSMAX1 degradation by SL-responsive PjKAI2d proteins. To test this idea, we co-expressed *PjKAI2d2* and *PjKAI2d3.2* with the SL-responsive genes *PjKAI2d1* and *PjKAI2d4* and tested the PjSMAX1.1 degradation response to different concentrations of *rac*-strigol.

Expression of *PjKAI2d1* and *PjKAI2d4* alone conferred significant reductions in the PjSMAX1.1 reporter ratio after treatment with *rac*-strigol concentrations as low as 1 to 10 nM, suggesting that the receptors encoded by these genes are highly sensitive to SL (**Fig. 3**). We then co-transformed *PjKAI2d2* or

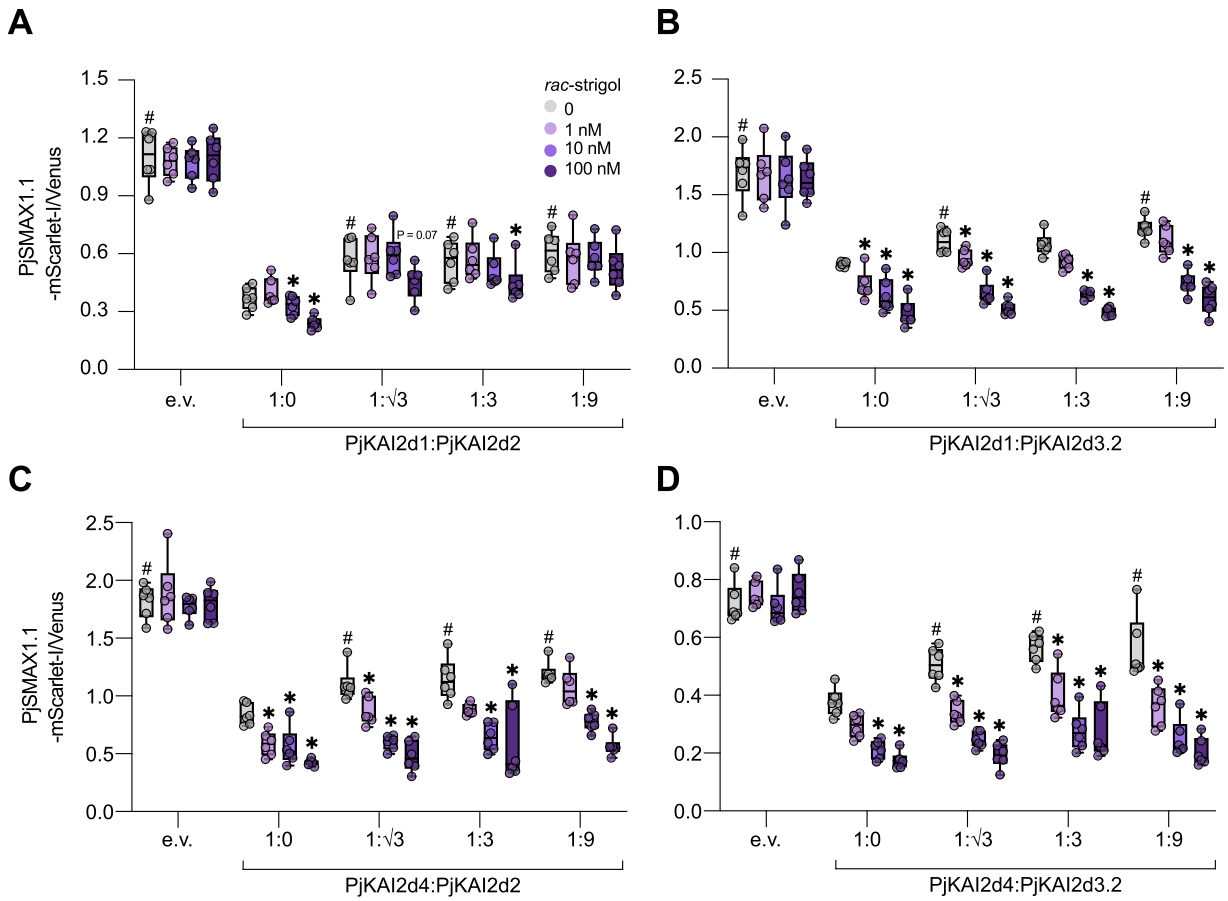

Fig. 3 Attenuation of PjSMAX1.1 degradation by PjKAI2d2 and PjKAI2d3.2. pRATIO1212-PjSMAX1.1 was co-transformed with varying ratios of *A. tumefaciens* cells carrying (A) *PjKAI2d1* and *PjKAI2d2*, (B) *PjKAI2d1* and *PjKAI2d3.2*, (C) *PjKAI2d4* and *PjKAI2d2* or (D) *PjKAI2d4* and *PjKAI2d3.2*. Final OD_{600} was brought to 1.2 with *A. tumefaciens* cells carrying an empty pGWB402 vector. Leaf discs were treated with 0.01% (v/v) acetone, 1 nM, 10 nM or 100 nM *rac*-strigol. e.v., pGWB402. $n = 6$ leaves per construct, mean ratio of 4–6 discs per leaf. $^{*}P < 0.05$, paired two-way ANOVA, comparison of treatments to acetone control with Bonferroni correction for multiple comparisons. $^{\#}P < 0.05$, one-way ANOVA with Bonferroni correction, comparison of acetone-treated controls to 1:0 ratio transformations. Box plot whiskers indicate minimum and maximum values.

PjKAI2d3.2 with *PjKAI2d1* or *PjKAI2d4* by mixing *A. tumefaciens* strains at different ratios. The amount of *A. tumefaciens* cells carrying *PjKAI2d1* or *PjKAI2d4* plasmids was kept constant, and supplementation with an empty vector strain was used to keep the overall concentration of *A. tumefaciens* cells used in each agroinfiltration of *N. benthamiana* leaves the same.

Co-transformation of *PjKAI2d1* cells with a 1:9 concentration of *PjKAI2d2* cells blocked degradation of the PjSMAX1.1 reporter in the presence of 10 nM or 100 nM *rac*-strigol treatments (**Fig. 3A**). At lower ratios of *PjKAI2d1* to *PjKAI2d2*, the response to 10 nM, but not 100 nM, *rac*-strigol was blocked. A similar effect was observed in 1:3 and 1:9 mixtures of *PjKAI2d1* and *PjKAI2d3.2* cells; degradation of the PjSMAX1.1 reporter after 1 nM *rac*-strigol treatment was blocked, but higher concentrations of *rac*-strigol overcame the inhibitory effect of *PjKAI2d3.2* co-expression (**Fig. 3B**). When PjKAI2d4 was used as the SL receptor, PjSMAX1.1 reporter degradation by 1 nM rac-strigol was inhibited by 1:3 and 1:9 mixtures with PjKAI2d2, and PjKAI2d3.2 did not block responses to any concentration of *rac*-strigol (**Fig. 3C, D**). This suggested that PjKAI2d4 activity was less affected than PjKAI2d1 by co-expression of *PjKAI2d2* and *PjKAI2d3.2*, perhaps because PjKAI2d4 is more sensitive to SL than PjKAI2d1. However, it is notable that in almost all cases, the addition of *PjKAI2d2* or *PjKAI2d3.2* caused a significant increase in the PjSMAX1.1 reporter ratio in mock-treated leaf disks compared to *PjKAI2d1* or *PjKAI2d4* alone (**Fig. 3**). Overall, these observations suggest that PjKAI2d2 and PjKAI2d3.2 inhibit SL signaling by PjKAI2d1 and PjKAI2d4 at low concentrations of SL, whether endogenous or applied. Therefore, PjKAI2d2 and PjKAI2d3.2 may shift the dynamic range of SL perception.

The catalytic triad is required for attenuation of SL signaling by PjKAI2d2 and PjKAI2d3.2

The serine residue of the Ser–His–Asp catalytic triad is required for the enzymatic and signaling functions of D14 and KAI2 pro-

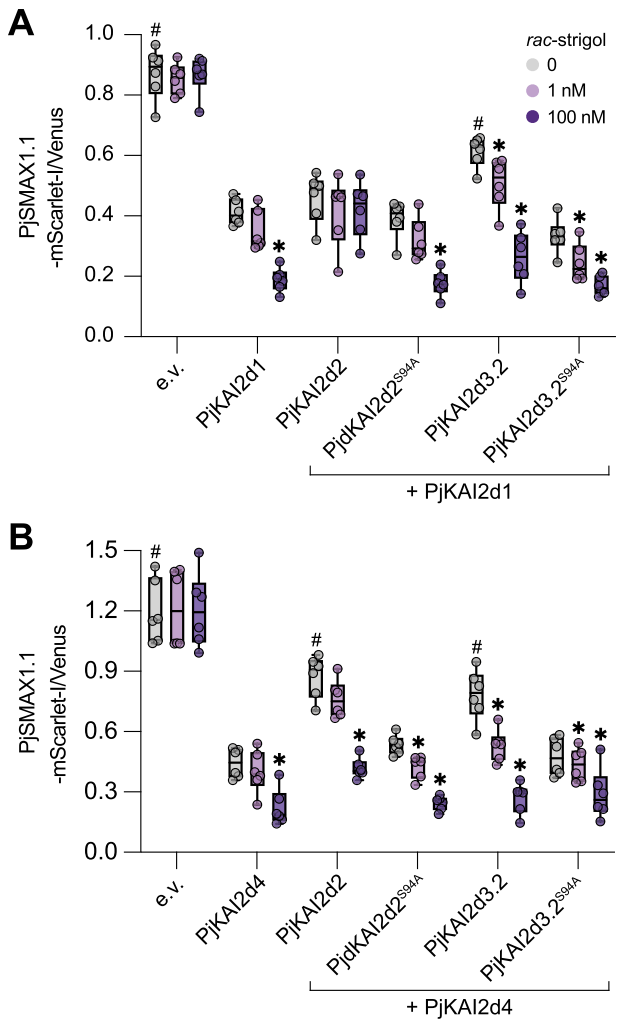

Fig. 4 Catalytic serine is required for PjKAI2d2 and PjKAI2d3.2 attenuation effects. PjSMAX1.1 was co-transformed with mixtures (1:9) of *A. tumefaciens* cells carrying (A) PjKAI2d1 or (B) PjKAI2d4 with PjKAI2d2 or PjKAI2d3.2 and the S94A catalytic mutant for each. Final OD_{600} was brought to 1.2 with *A. tumefaciens* cells carrying an empty pGWB402 vector. Leaf discs were treated with 0.01% (v/v) acetone and 1 nM or 100 nM *rac*-strigol. e.v., pGWB402. $n = 6$ leaves per construct, mean ratio of 4–6 discs per leaf. $^{*}P < 0.05$, paired two-way ANOVA, comparison of treatments to acetone control with Bonferroni correction for multiple comparisons. $^{\#}P < 0.05$, one-way ANOVA with Bonferroni correction, comparison of acetone-treated controls to PjKAI2d2 or PjKAI2d4 1:0 ratio transformations. Box plot whiskers indicate minimum and maximum values.

teins (Hamiaux et al. 2012, Waters et al. 2015a, 2015b, Yao et al. 2018, Seto et al. 2019). Therefore, we replaced the catalytic serine with alanine of PjKAI2d2 and PjKAI2d3.2 and tested whether PjKAI2d2^{S94A} and PjKAI2d3.2^{S94A} mutant proteins can inhibit the SL-induced degradation of PjSMAX1.1 by PjKAI2d1 or PjKAI2d4. Co-transformation of *PjKAI2d1* and *PjKAI2d2* (1:9) blocked the degradation of the PjSMAX1.1 reporter by 1 nM or 100 nM *rac*-strigol treatments (**Fig. 4A**). In contrast, co-transformation of *PjKAI2d2*^{S94A} with *PjKAI2d1* had no effect on SL-induced degradation of PjSMAX1.1 reporter compared to *PjKAI2d1* alone. This result indicates that PjKAI2d2 requires hydrolytic activity to inhibit PjSMAX1.1 degradation. Co-transformation of *PjKAI2d1* and *PjKAI2d3.2* (1:9) had a different effect than *PjKAI2d2*. *PjKAI2d3.2* caused a significant increase in the PjSMAX1.1 reporter ratio in mock-treated leaf disks, implying that it inhibited PjSMAX1.1 degradation caused by endogenous SLs. As noted earlier, *PjKAI2d3.2* appeared to shift the dynamic range of the PjSMAX1.1 degradation response to SL (**Figs. 3B**, **4A**). In contrast, this effect was not observed from co-expression of *PjKAI2d3.2*^{S94A}. Similar trends were obtained when *PjKAI2d2* and *PjKAI2d3.2* were co-transformed with *PjKAI2d4* (**Fig. 4B**). Both *PjKAI2d2* and *PjKAI2d3.2* caused an increase in the baseline PjSMAX1.1 reporter ratio, and their effects on the dynamic range of SL-induced PjSMAX1.1 degradation were dependent on the catalytic serine. These phenomena suggest that *PjKAI2d2* and *PjKAI2d3.2* are not pseudogenes; instead, these paralogs appear to have dominant-negative effects.

Striga hermonthica also has dominant-negative KAI2d paralogs

We investigated whether this mechanism of SL signaling attenuation may occur in other parasitic plants. Prior studies have shown that three divergent *KAI2* transgenes from the obligate hemiparasite *S. hermonthica*—*ShKAI2d2*, *ShHTL10* and *ShHTL11*—do not confer SL responses to *A. thaliana* in cross-species complementation assays (Conn et al. 2015, Toh et al. 2015). Nonetheless, the affinity of ShHTL10 and ShHTL11 for different SLs in vitro is comparable or in some cases even higher than the extraordinarily SL-sensitive receptor ShHTL7 (Tsuchiya et al. 2015, Wang et al. 2021). These three genes are part of a distinct clade from the *KAI2d* genes in *S. hermonthica* that are known to be active in transgenic assays (**Fig. 5**).

We tested whether ShHTL10 and ShHTL11 are able to trigger degradation of the PjSMAX1.1 reporter in response to SL in *Nicotiana benthamiana* assays. Neither gene affected the abundance of the PjSMAX1.1 reporter in either the presence or absence of *rac*-strigol relative to an empty vector control (**Fig. 6A**). In contrast, ShHTL7 caused a strong reduction in the abundance of PjSMAX1.1 reporter under mock-treated conditions and further reduced it under *rac*-strigol treatment. Therefore, ShHTL10 and ShHTL11 act similar to PjKAI2d2, PjKAI2d3 and PjKAI2d3.2 in this assay.

This led us to test whether co-expression of ShHTL11, which has higher affinity for strigol than ShHTL10, with ShHTL7 attenuates the SL-responsive degradation of SMAX1 (Tsuchiya et al. 2015). We found that increasing the ratio of *A. tumefaciens* carrying *ShHTL11* relative to *A. tumefaciens* carrying *ShHTL7* during agroinfiltration led to an increase in the abundance of PjSMAX1.1 reporter under mock-treated conditions (**Fig. 6B**). At the highest ratio (1:9 *ShHTL7* to *ShHTL11* cells), we observed a clear difference in the response to 10 nM *rac*-strigol compared to 1 nM *rac*-strigol that was not present when *ShHTL11*

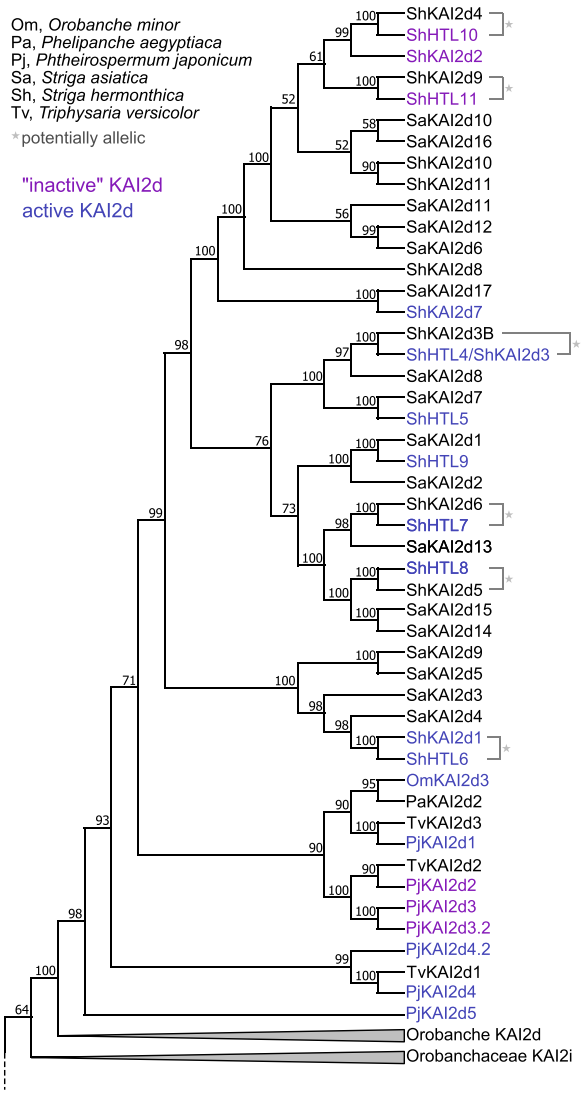

Fig. 5 Phylogenetic analysis of KAI2 proteins in parasitic plants. Cladogram of KAI2d proteins in parasitic Orobanchaceae. Full phylogeny of KAI2 proteins is shown in **Supplementary Figs. S1, S2**. Parasitic KAI2d proteins that have shown SL signaling activity in heterologous plant assays (e.g. cross-species complementation of *A. thaliana* or SMAX1 reporter degradation in *N. benthamiana*) are considered active (blue); those that have not shown SL signaling activity are termed 'inactive' (purple) but may have alternative activities such as SL signaling attenuation. Activities were reported in Conn et al. (2015), Toh et al. (2015) and Takei et al. (2023) (**Fig. 2**). Stars indicate *S. hermonthica KAI2d* gene annotations (Conn et al. 2015, Toh et al. 2015) that may be allelic. These *KAI2d* genes had an average of 0 substitutions per site in the phylogenetic construction and more than 97% amino acid and nucleotide identity. Bootstrap values, shown, were calculated using UltraFast (10,000 iterations). Branches are not scaled.

was absent. These data indicate that *ShHTL11* can cause a shift in the dynamic range of SL responses, similar to *PjKAI2d2* and *PjKAI2d3.2*.

Discussion

The prevailing model for host detection in parasitic plants is that KAI2d proteins sensitively perceive SLs in the rhizosphere and initiate responses such as seed germination or chemotropic root growth that improve the likelihood of successful attachment to a host root (Nelson 2021, Kee et al. 2023). We found examples of three *KAI2d* genes in *P. japonicum*—PjKAI2d2, PjKAI2d3 and PjKAI2d3.2—that appear to be inactive in plant-based functional assays, similar to *ShKAI2d2, ShHTL10* and *ShHTL11* from *S. hermonthica* (Conn et al. 2015, Toh et al. 2015). It is notable that *PjKAI2d2* and *PjKAI2d3.2*, but not *PjKAI2d3*, conferred very weak but statistically significant responses to *rac*-strigol in germination assays of transgenic *Arabidopsis d14 kai2* seed (Ogawa et al. 2022). It may be that PjKAI2d2 and PjKAI2d3.2 have a highly reduced ability to trigger SMAX1 degradation, but are not entirely unable to do so as suggested by our assays in *N. benthamiana* (**Fig. 2**). This discrepancy could arise from differences in the relative abundance of SMAX1 versus PjKAI2d proteins in each system.

Our observations of the activity of PjKAI2d proteins align well with those of a concurrent study (Takei et al. 2024). In cross-species complementation assays of *PjKAI2d* genes expressed in an *A. thaliana kai2* mutant, *PjKAI2d4* conferred extremely sensitive germination responses to *rac*-GR24 that were comparable to *ShHTL7* from *S. hermonthica* and *OmKAI2d3* from *O. minor*. To a lesser degree, *PjKAI2d5* and *PjKAI2d1* also conferred germination responses to *rac*-GR24. On the other hand, *PjKAI2d2, PjKAI2d3* and *PjKAI2d3-2* (a slightly different sequence than PjKAI2d3.2) showed little or no activity. In yeast two-hybrid assays, *rac*-GR24 induced protein–protein interactions between PjKAI2d2, but not PjKAI2d3 or PjKAI2d3-2, and SMAX1 from *Arabidopsis* and *P. japonicum* (Takei et al. 2024). This might explain why PjKAI2d3 and PjKAI2d3-2, at least, are unable to trigger SMAX1 degradation (**Fig. 2**).

Interestingly, phylogenetic analysis separates *KAI2d* genes from *P. japonicum* and *S. hermonthica* into subclades of 'inactive' and SL-responsive paralogs (**Fig. 5**). We hypothesize that the 'inactive' *KAI2d* are not pseudogenes, but instead have adaptive value as antagonists of SL signaling. This is based upon the observations that *PjKAI2d2* and *PjKAI2d3.2* are highly expressed in *P. japonicum* seedlings, show expression patterns that are consistent with feedback regulation (i.e. expression positively correlates with activation of SL signaling) and inhibit SL-induced degradation of PjSMAX1.1 protein in a manner that requires an active catalytic triad (Ogawa et al. 2022) (**Figs. 3**, **4**). Similarly, ShHTL10 and ShHTL11 are able to bind SLs but do not transduce positive responses to SLs (Tsuchiya et al. 2015, Toh et al. 2015, Wang et al. 2021; **Fig. 6**). The expression pattern of *ShHTL10* and *ShHTL11* has not been well-characterized, but semi-quantitative RT-PCR has suggested that both genes are expressed in seeds (Tsuchiya et al. 2015). In another study, the putatively equivalent genes *ShKAI2d4* and *ShKAI2d9* showed seedling-specific expression that declined after host infection (Ogawa et al. 2022). It is also notable that the

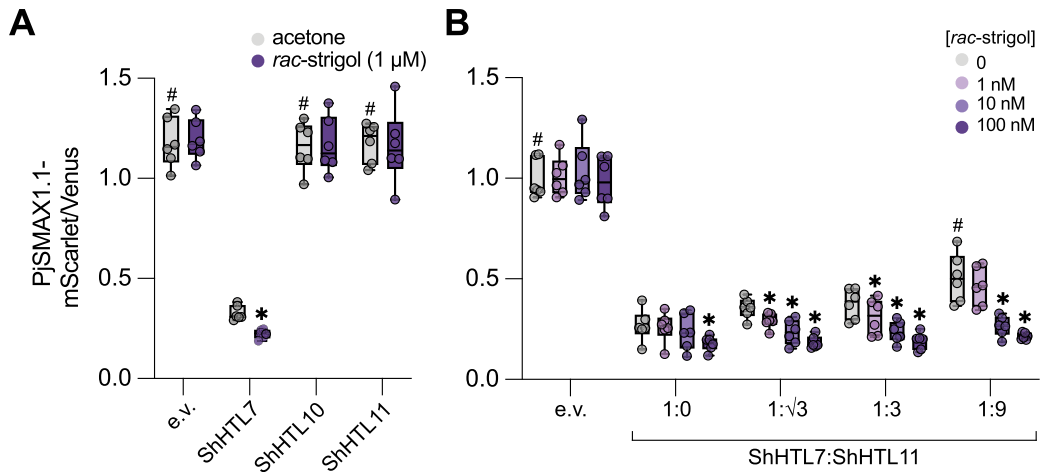

Fig. 6 Effects of ShHTL proteins on PjSMAX1.1 degradation. Analysis of PjSMAX1.1 ratiometric reporter co-transformed with pGWB402-ShHTL constructs in *Nbd14a,b kai2i* leaves. Co-transformed leaf discs were treated with 0.01% (v/v) acetone or 1 μM *rac*-strigol. (B) pRATIO1212-PjSMAX1.1 was co-transformed with *A. tumefaciens* cells carrying *ShHTL7* and varying ratios of *A. tumefaciens* cells carrying *ShHTL11*. Final OD_{600} was brought to 1.2 with *A. tumefaciens* cells carrying an empty pGWB402 vector. Leaf discs were treated with 0.01% (v/v) acetone and 1 nM, 10 nM or 100 nM *rac*-strigol. e.v., pGWB402 empty vector. For both experiments, $n = 6$ leaves per construct, mean ratio of 4–6 discs per leaf. $^{*}P < 0.05$, paired two-way ANOVA, comparison of treatments to acetone control with Bonferroni correction for multiple comparisons. $^{\#}P < 0.05$, one-way ANOVA with Bonferroni correction, comparison of acetone-treated controls to 1:0 ratio transformations. Box plot whiskers indicate minimum and maximum values.

closest homologs of *ShHTL10* and *ShHTL11* in *Striga asiatica* (i.e. *SaKAI2d10*, *SaKAI2d16*, *SaKAI2d6*, *SaKAI2d11* and *SaKAI2d12*) show enriched expression in seedlings, much like the 'inactive' *PjKAI2d* genes, and therefore may play more significant roles post-germination (Yoshida et al. 2019).

How dominant-negative KAI2d proteins might work

We do not yet know how PjKAI2d2 and PjKAI2d3.2 proteins may attenuate SL signaling, but at least two mechanisms seem plausible. One possibility is that these proteins have mutations that allow them to interact with only one signaling partner, SCF^{MAX2} or SMAX1, but not both. This could competitively sequester key components of KAI2-dependent signaling, reducing the ability of proteins like PjKAI2d1 and PjKAI2d4 to trigger polyubiquitination and degradation of SMAX1 in response to SL perception. Surface residues involved in interaction with MAX2 are normally well-conserved among KAI2 and D14 proteins (Bythell-Douglas et al. 2017). In PjKAI2d2 and PjKAI2d3.2 proteins, by contrast, these residues are not conserved, suggesting that interactions with MAX2 may be disrupted (**Fig. 7**). It should be noted, however, that amino acid substitutions at the KAI2 interface with MAX2 may sometimes strengthen, rather than weaken, KAI2–MAX2 protein–protein interactions (Guercio et al. 2024).

An alternative possibility is that these proteins may be unable to interact with either SCF^{MAX2} or SMAX1 and instead function as hydrolases that degrade SL. Indirectly supporting this idea, ShHTL10 and ShHTL11 bind and/or hydrolyze SLs in vitro, potentially with a greater affinity than ShHTL7 in some cases, but do not show SL-induced interactions with either MAX2 or SMAX1 in yeast two-hybrid assays (Tsuchiya et al. 2015, Wang et al. 2021). It is not clear if ShHTL10 and ShHTL11 are capable of weak interactions with either MAX2 or SMAX1 that were not detectable under the high stringency selection that was used in these experiments (Wang et al. 2021). However, further support for a lack of interaction between ShHTL10 and ShHTL11 with MAX2 at least has been provided by in vitro pull-down assays (Wang et al. 2021).

At this time, we favor the idea that the dominant-negative effects of the 'inactive' KAI2d proteins arise from nonproductive, competitive interactions with KAI2 signaling partners rather than SL hydrolysis. We note that constitutive expression of *PjKAI2d2* in *P. japonicum* hairy roots increases chemotropic responses to SL, while constitutive expression of $PjKAI2d2^{R183H}$ blocks chemotropism (Ogawa et al. 2022). Arg183 is a surface residue that is well-conserved in KAI2 and D14 proteins. In *Arabidopsis* and rice D14, the R183H mutation (R233H equivalent in OsD14) disrupts D14 interactions with SMXL7 in yeast two-hybrid assays, but has no effect on SL hydrolysis activity (Seto et al. 2019). Thus, the functional differences between D14 and $D14^{R183H}$ are not due to changes in SL hydrolysis capacity and are more likely a consequence of changes to D14 protein–protein interactions that affect SL signal transduction. If the R183H mutation has an equivalent effect on PjKAI2d2 function, then the opposite effects of PjKAI2d2 and $PjKAI2d2^{R183H}$ on chemotropism are likely due to differences in protein–protein interactions (e.g. with SMAX1) rather than SL degradation. However, we must be clear that the hypothesized effect of

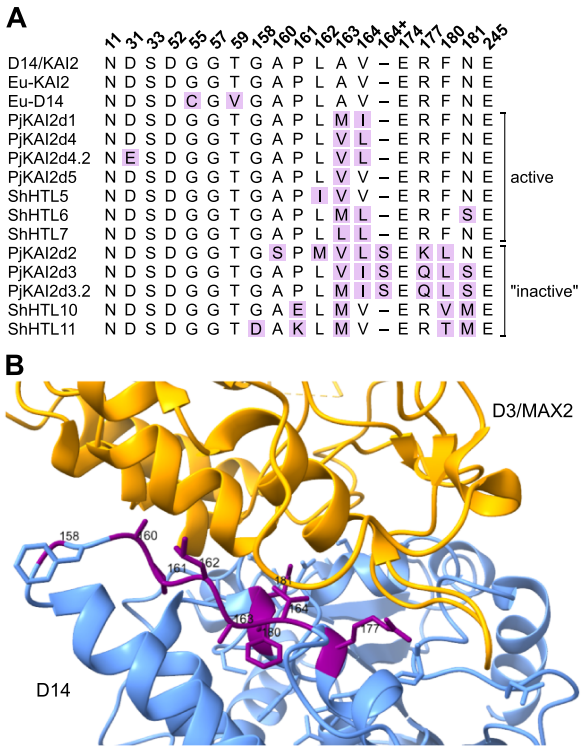

Fig. 7 PjKAI2d amino acid identities at the MAX2 interface. (A) Amino acid identities of parasite KAI2d proteins at residues important for D14–D3/MAX2 interaction as determined by Yao et al. (2016). Residues highlighted in purple indicate differences from the highly conserved consensus residues of D14/KAI2, Eu-KAI2 and Eu-D14 protein classes (Bythell-Douglas et al. 2017). Residue numbers are based on *A. thaliana* D14 (Yao et al. 2016). Residue 164+ is an extra residue found in PjKAI2d2, PjKAI2d3 and PjKAI2d3.2 with no corresponding residue in AtD14. Parasitic KAI2d proteins that have shown SL signaling activity in heterologous plant assays (e.g. cross-species complementation of *A. thaliana* or SMAX1 reporter degradation in *N. benthamiana*) are considered active; those that have not shown SL signaling activity are termed 'inactive' but may actually have alternative activities such as SL signaling attenuation. (B) Three-dimensional protein structure of the AtD14–D3-ASK1 complex from Protein Data Bank model 5HZG (Yao et al. 2016). Non-consensus residues from (A) in at least one 'inactive' PjKAI2d or ShHTL protein are shaded. AtD14 structure, blue, bottom; D3/MAX2 structure, orange, top.

the R183H substitution has not been tested through biochemical characterization (e.g. SL hydrolysis and protein–protein interaction assays) of PjKAI2d2 and PjKAI2d2^{R183H}. Therefore, this interpretation of the data is only tentative.

The potential adaptive value of attenuated SL signaling

KAI2d proteins that attenuate SL signaling could be advantageous to root parasitic plants. For example, inhibitory responses to SLs that are indicative of a non-host could prevent suicidal germination (Nelson 2021). Feedback inhibition of SL responses could also be important for chemotropic growth toward a host root by preventing SL signaling systems from becoming saturated and losing orientation. The so-called 'perfectly adapted' chemotropic or chemotactic systems are able to sense a concentration gradient of a signal rather than an absolute concentration (Levchenko and Iglesias 2002, Arkowitz 2009, Insall et al. 2022). However, this is challenging to achieve; because of their small sizes, the different sides of cells or tissues typically experience very shallow gradients of a diffusible signal. Several strategies have evolved to increase the steepness of a signal gradient. First, the organism or cells may destroy the signal locally. This 'self-guiding' or 'self-generating' approach to chemotropism or chemotaxis reduces the amount of signal in the immediate environment to prevent saturation of the receptors and create a local gradient. Second, the amount of available receptor may be adjusted through transport to or from the site of perception or changes in the rates of receptor synthesis or degradation. Third, asymmetric spatial distribution of the receptor or signaling machinery may be used to improve perception of a shallow gradient (Levchenko and Iglesias 2002, Arkowitz 2009, Insall et al. 2022).

Regardless of how *PjKAI2d2* and *PjKAI2d3.2* work, their expression patterns suggest how and when the SL signaling attenuation mechanism is used. These genes are highly expressed in seedlings compared to other *PjKAI2d* paralogs, suggesting that they are more important for seedling growth than germination (Ogawa et al. 2022). In addition, these genes are induced by *rac*-strigol. This change in expression may indicate a negative feedback mechanism: as PjSMAX1 is degraded, putatively in response to *rac*-strigol perception by PjKAI2d1 PjKAI2d4, and PjKAI2d5, the expression of *PjKAI2d2* and *PjKAI2d3.2* increases. PjKAI2d2 and PjKAI2d3.2 activity could then reduce SL signaling locally to make it easier for the root to detect an SL gradient (**Fig. 8**). This model may explain why overexpression of *PjKAI2d2* in *P. japonicum* led to an increase in the frequency of chemotropic root growth toward SL (Ogawa et al. 2022). Finally, expression of these genes is downregulated by nutrients (or upregulated by nutrient deprivation) (Ogawa et al. 2022). This could keep chemotropic growth from occurring when there is no benefit to seeking a host root and engaging in parasitism.

Materials and Methods

Plant growth conditions

Nicotiana benthamiana seeds were incubated at −80°C for 12 h, germinated on Sungro Professional Growing Mix and supplemented with Gnatrol WDG, Marathon (imidacloprid) and Osmocote 14-14-14 fertilizer. Seedlings were transferred to pots at ∼7–10 d old. *Nicotiana benthamiana* plants were grown under long-day conditions (16 h white light, 120 μmol m^{-2} s^{-1}; 8 h dark) at ∼22°C.

Gene editing

gRNAs to target *NbKAI2* genes were designed manually. Both gRNA-encoding genes were cloned into a single pHEE401E construct as described previously, but with Q5 high-fidelity DNA polymerase (New England Biolabs, Ipswich, MA) and NEBridge Golden Gate Assembly Kit (BsaI-HF v2, New England Biolabs) (Xing et al. 2014, Wang et al. 2015b, White et al. 2022). Transformation of

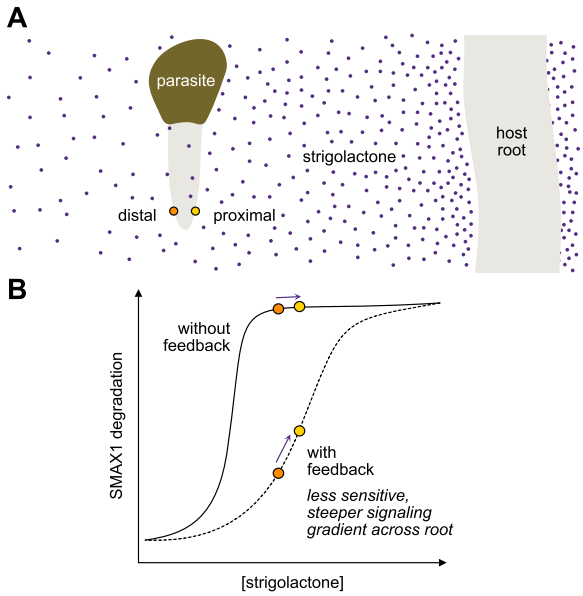

Fig. 8 Model for SL signaling attenuation during parasite chemotropism. (A) SLs (purple dots) exuded from a host root putatively decrease in concentration at increasing distances from the root. Chemotropic growth toward the host root may require a nascent parasitic seedling to differentiate between very similar SL concentrations at the host-proximal and host-distal sides of its root. (B) SL perception in parasitic seeds and seedlings putatively causes degradation of SMAX1. Feedback inhibition or attenuation of SL signaling by proteins such as PjKAI2d2 and PjKAI2d3.2 reduces responses to low concentrations of SL (dashed line). This could allow the parasitic seedling to experience a steeper SL signaling gradient across the proximal (orange circle, left) and distal (yellow circle, right) sides of the root, allowing orientation toward the host based on differential SMAX1 degradation, at the expense of SL sensitivity.

Nbd14a,b was performed by the Plant Transformation Facility at the University of California, Davis, as described previously (White et al. 2022).

Genotyping

DNA was extracted from *N. benthamiana* leaf tissue ground in liquid N_2 and incubated with 250 μl of buffer (0.35 M sorbitol, 5 mM EDTA, 100 mM Tris-Cl) and kept at 4°C for 20 min. Tissue mixtures were centrifuged for 10 min at 6000 rpm at 4°C. The pellet was resuspended with 350 μl of lysis buffer (250 mM NaCl, 25 mM EDTA, 200 mM Tris-Cl, 0.5% SDS). Lysate was incubated at 95°C for 15 min, and then 400 μl of ice-cold 100% isopropanol was added. Lysate was centrifuged for 10 min at 12,000 rpm. Pellet was washed in 400 μl of ice-cold 70% ethanol, centrifuged for 5 min at 12,000 rpm and ethanol was removed. DNA was air dried and resuspended with 50 μl of buffer (10 mM Tris-HCl, 1 mM EDTA, pH 8). Genotyping was performed with Taq polymerase (New England Biolabs) using standard PCR reaction conditions supplemented with $MgCl_2$ and primers described in **Supplementary Table S1**.

PjSMAX1 degradation assays

Gateway entry clones containing each CDS of *PjKAI2d2*, *PjKAI2d3* and *PjKAI2d3.2* were previously described (Ogawa et al. 2022). Each CDS of *PjSMAX1.1* and *PjSMAX1.2* CDS was PCR-amplified and cloned into pENTR D-TOPO entry vector to generate entry vectors and then cloned into the pRATIO1212 ratiometric reporter vector (Khosla et al. 2020b). *Agrobacterium tumefaciens* GV3101 that also carries a plasmid expressing p19, suppressor of gene-silencing, was transformed with pRATIO1212-SMAX1.1 and pRATIO1212-SMAX1.2 by electroporation. The CDSs for *KAI2d* genes were synthesized (Twist Bioscience, South San Francisco, CA). The CDSs for *PjKAI2d1*, *PjKAI2d4*, *PjKAI2d4.2* and *PjKAI2d5* (Ogawa et al. 2022); *OcKAI2d1* (Larose et al. 2022); and *ShHTL7*, *ShHTL10* and *ShHTL11* (Toh et al. 2015) were previously described. CDSs were Gateway cloned into an ampicillin-resistant pDONR221 entry vector and Sanger sequence verified. PjKAI2d2^{S94A} and PjKAI2d3.2^{S94A} ampicillin-resistant pDONR221 entry vectors were created using a Q5 Site-Directed Mutagenesis kit (New England Biolabs). The *KAI2d* CDSs were transferred into the plant transformation vector pGWB402 (Nakagawa et al. 2007) using Gateway LR cloning (Invitrogen, Waltham, MA). pGWB402-KAI2d vectors were transformed into *A. tumefaciens* strain GV3101 via electroporation. Transient transformation of *N. benthamiana* and measurement of mScarlet-I and Venus were performed as described previously (Khosla and Nelson 2020), with the following modifications for the cell densities of *A. tumefaciens* cultures resuspended in infiltration media prior to injection of *N. benthamiana* leaves: **Figs. 1, 2, 6A**, *A. tumefaciens* containing pRATIO1212-*PjSMAX1* vectors was injected at an optical density at 600 nm wavelength (OD_{600}) of 0.8. **Figure 2**, *A. tumefaciens* containing *KAI2lHTL* vectors or pGWB402 alone was injected at an OD_{600} of 0.1. **Figures 3, 4**, *A. tumefaciens* containing pRATIO1212-*PjSMAX1.1* was injected at an OD_{600} of 0.7 and *A. tumefaciens* containing *PjKAI2d1*, *PjKAI2d4* and *ShHTL7* vectors was injected at an OD_{600} of 0.05. Final OD_{600} was brought to 1.2 with *A. tumefaciens* containing empty vector (pGWB402). **Figures 3, 6B**, *A. tumefaciens* containing *PjKAI2d2*, *PjKAI2d3.2* and *ShHTL11* vectors was injected at OD_{600} values of 0.087, 0.15 or 0.45. **Figure 4**, *A. tumefaciens* containing *PjKAI2d2* and *PjKAI2d3.2* vectors was injected at an OD_{600} of 0.45. Racemic GR24 and racemic strigol were synthesized by StrigoLab (Torino, Italy). KAR_1 was synthesized and kindly supplied by Dr. Adrian Scaffidi and Dr. Gavin Flematti (University of Western Australia, Crawley, Australia). Treatments of excised leaf disks per each assay are as follows: **Fig. 1**, 0.02% (v/v) acetone, 10 μM *rac*-GR24, 10 μM KAR_1; **Figs. 1, 2A**, 0.02% (v/v) acetone or 10 μM *rac*-GR24; **Figs. 2B, 6A**, 0.01% (v/v) acetone or 1 μM *rac*-strigol; **Figs. 3, 6B**, 0.01% (v/v) acetone, 1 nM *rac*-strigol, 10 nM *rac*-strigol or 100 nM *rac*-strigol; and **Fig. 4**, 0.01% (v/v) acetone, 1 nM *rac*-strigol or 100 nM *rac*-strigol. Fluorescence was read ∼16 h post-treatment. Each data point represents the average ratio of mScarlet-I to Venus fluorescence of 4–8 leaf disks from a single transformed leaf ($n = 4–7$ leaves).

Phylogenetic analysis

KAI2 sequences were collected from published datasets (Conn et al. 2015, Toh et al. 2015, Yoshida et al. 2019, Stirling et al. 2024) (**Supplementary Tables S2 and S3**). Protein sequence alignments were performed in MEGA 11 using the MUSCLE multiple sequence alignment algorithms (Tamura et al. 2021). The multiple sequence alignment was trimmed using ClipKIT 'smart-gap' (Steenwyk et al. 2020). Ninety-six out of 400 positions were trimmed. The phylogenetic tool IQ TREE inferred the evolutionary history using the maximum likelihood method and JTT matrix-based model (Trifinopoulos et al. 2016). The tree with the highest negative log likelihood was selected. The gamma model was used to estimate evolutionary rate differences among sites (eight categories). The alpha parameter was estimated from the dataset. There were a total of 304 amino acid positions and 228 sequences in the final dataset. Bootstrap values were calculated using UltraFast (10,000 iterations). Tree search settings were 0.5 perturbation strength and 100 iterations to stop. Tree was viewed in MEGA 11 (Tamura et al. 2021). The branches are not scaled in **Fig. 5**.

Statistical analysis and data presentation

All data were analyzed, and graphs were produced using Prism 10 (GraphPad) with figure assembly in Affinity Designer.

Supplementary Data

Supplementary data are available at *PCP* online.

Data Availability

Raw data, plasmids and seeds of the *N. benthamiana Nbd14a,b kai2* mutant are freely available upon request with a Material Transfer Agreement.

Funding

National Science Foundation (NSF-IOS 1856741 to D.C.N.; NSF Research Traineeship Program Grant DGE-1922642 'Plants3D' to A.R.F.W. and A.K.), the US Department of Agriculture (Hatch project CA-R-BPS-5209-H to D.C.N., NIFA AFRI Predoctoral Fellowship 2023-67011-319 40396 to A.K.), the Japan Society for the Promotion of Science (JSPS) KAKENHI Grants-in-Aid for JSPS Fellows (22KJ3127 to S.O.), and the Ministry of Education, Culture, Sports, Science and Technology KAKENHI grant (20H05909 to K.S.)

Acknowledgments

We thank the UC Davis Plant Transformation Facility for *N. benthamiana* transformation services and the UC Riverside Genomics Core Facility for DNA sequencing services.

Author Contributions

A.R.F.W. and A.K. contributed to investigation, validation, formal analysis and visualization. A.R.F.W., S.O. and K.S. contributed to resources. A.R.F.W. and D.C.N. contributed to project administration. Original manuscript draft was prepared by A.R.F.W. and D.C.N. All authors contributed to manuscript review and editing. A.R.F.W., A.K., S.O., D.C.N. and K.S. contributed to funding acquisition. D.C.N. contributed to project conceptualization and supervision.

Disclosures

The authors have no conflicts of interest to disclose.

References

Arellano-Saab, A., Bunsick, M., Al Galib, H., Zhao, W., Schuetz, S., Bradley, J.M., et al. (2021) Three mutations repurpose a plant karrikin receptor to a strigolactone receptor. *Proc. Natl. Acad. Sci. U.S.A.* 118: e2103175118.

Arkowitz, R.A. (2009) Chemical gradients and chemotropism in yeast. *Cold Spring Harb. Perspect. Biol.* 1: a001958.

Blázquez, M.A., Nelson, D.C. and Weijers, D. (2020) Evolution of plant hormone response pathways. *Annu. Rev. Plant Biol.* 71: 327–353.

Bombarely, A., Rosli, H.G., Vrebalov, J., Moffett, P., Mueller, L.A. and Martin, G.B. (2012) A draft genome sequence of Nicotiana benthamiana to enhance molecular plant-microbe biology research. *Mol. plant-microb. interact.* 25: 1523–1530.

Bouwmeester, H., Li, C., Thiombiano, B., Rahimi, M. and Dong, L. (2021) Adaptation of the parasitic plant lifecycle: germination is controlled by essential host signaling molecules. *Plant Physiol.* 185: 1292–1308.

Bunsick, M., Xu, Z., Pescetto, G., Ly, G., Hountalas, J., Boyer, F.-D., et al. (2022) HTL/KAI2 signalling substitutes for light to control plant germination. *bioRxiv*.

Bythell-Douglas, R., Rothfels, C.J., Stevenson, D.W.D., Graham, S.W., Wong, G.K.-S., Nelson, D.C., et al. (2017) Evolution of strigolactone receptors by gradual neo-functionalization of KAI2 paralogues. *BMC Biol.* 15: 52.

Carbonnel, S., Torabi, S., Griesmann, M., Bleek, E., Tang, Y., Buchka, S., et al. (2020) Lotus japonicus karrikin receptors display divergent ligand-binding specificities and organ-dependent redundancy. *PLoS Genet.* 16: e1009249.

Clark, J., Bennett, T. and Waters, M. (2024) Cracking the enigma: understanding strigolactone signalling in the rhizosphere. *J. Exp. Bot.* 75: 1159–1173.

Conn, C.E., Bythell-Douglas, R., Neumann, D., Yoshida, S., Whittington, B., Westwood, J.H., et al. (2015) PLANT EVOLUTION. Convergent evolution of strigolactone perception enabled host detection in parasitic plants. *Science* 349: 540–543.

Conn, C.E. and Nelson, D.C. (2015) Evidence that KARRIKIN-INSENSITIVE2 (KAI2) receptors may perceive an unknown signal that is not Karrikin or Strigolactone. *Front. Plant Sci.* 6: 1219.

Cook, C.E., Whichard, L.P., Turner, B., Wall, M.E. and Egley, G.H. (1966) Germination of witchweed (Striga lutea Lour.): isolation and properties of a potent stimulant. *Science* 154: 1189–1190.

de Saint Germain, A., Jacobs, A., Brun, G., Pouvreau, J.-B., Braem, L., Cornu, D., et al. (2021) A Phelipanche ramosa KAI2 protein perceives strigolactones and isothiocyanates enzymatically. *Plant Commun.* 2: 100166.

Dor, E., Plakhine, D., Joel, D.M., Larose, H., Westwood, J.H., Smirnov, E., et al. (2020) A new race of sunflower broomrape (Orobanche cumana) with a wider host range due to changes in seed response to strigolactones. *Weed Sci.* 68: 134–142.

Fernández-Aparicio, M., Flores, F. and Rubiales, D. (2009) Recognition of root exudates by seeds of broomrape (Orobanche and Phelipanche) species. *Ann. Bot.* 103: 423–431.

Fernández-Aparicio, M., Yoneyama, K. and Rubiales, D. (2011) The role of strigolactones in host specificity of Orobanche and Phelipanche seed germination. *Seed Sci. Res.* 21: 55–61.

Flematti, G.R., Ghisalberti, E.L., Dixon, K.W. and Trengove, R.D. (2004) A compound from smoke that promotes seed germination. *Science* 305: 977.

Guercio, A.M., Gilio, A.K., Pawlak, J. and Shabek, N. (2024) Structural insights into rice KAI2 receptor provide functional implications for perception and signal transduction. *J. Biol. Chem.* 300: 107593.

Hamiaux, C., Drummond, R.S.M., Janssen, B.J., Ledger, S.E., Cooney, J.M., Newcomb, R.D., et al. (2012) DAD2 is an α/β hydrolase likely to be involved in the perception of the plant branching hormone, strigolactone. *Curr. Biol.* 22: 2032–2036.

Huet, S., Pouvreau, J.-B., Delage, E., Delgrange, S., Marais, C., Bahut, M., et al. (2020) Populations of the parasitic plant *Phelipanche ramosa* influence their seed microbiota. *Front. Plant Sci.* 11: 1075.

Insall, R.H., Paschke, P. and Tweedy, L. (2022) Steering yourself by the bootstraps: how cells create their own gradients for chemotaxis. *Trends Cell Biol.* 32: 585–596.

Jiang, L., Liu, X., Xiong, G., Liu, H., Chen, F., Wang, L., et al. (2013) DWARF 53 acts as a repressor of strigolactone signalling in rice. *Nature* 504: 401–405.

Kee, Y.J., Ogawa, S., Ichihashi, Y., Shirasu, K. and Yoshida, S. (2023) Strigolactones in rhizosphere communication: multiple molecules with diverse functions. *Plant Cell Physiol.* 64: 955–966.

Khosla, A., Morffy, N., Li, Q., Faure, L., Chang, S.H., Yao, J., et al. (2020a) Structure-function analysis of SMAX1 reveals domains that mediate its Karrikin-induced proteolysis and interaction with the receptor KAI2. *Plant Cell* 32: 2639–2659.

Khosla, A. and Nelson, D.C. (2020) Ratiometric measurement of protein abundance after transient expression of a transgene in Nicotiana benthamiana. *Biol. Protoc.* 10: e3747.

Khosla, A., Rodriguez-Furlan, C., Kapoor, S., Van Norman, J.M. and Nelson, D.C. (2020b) A series of dual-reporter vectors for ratiometric analysis of protein abundance in plants. *Plant Direct* 4: e00231.

Krupp, A., Bertsch, B. and Spring, O. (2021) Costunolide influences germ tube orientation in sunflower broomrape—a first step toward understanding chemotropism. *Front. Plant Sci*. 12: 699068.

Larose, H., Plakhine, D., Wycoff, N., Zhang, N., Conn, C., Nelson, D.C., et al. (2022) An Orobanche cernua x Orobanche cumana segregating population provides insight into the regulation of germination specificity in a parasitic plant. *bioRxiv*.

Levchenko, A. and Iglesias, P.A. (2002) Models of eukaryotic gradient sensing: application to chemotaxis of amoebae and neutrophils. *Biophys. J.* 82: 50–63.

Li, Q., Martín-Fontecha, E.S., Khosla, A., White, A.R.F., Chang, S., Cubas, P., et al. (2022) The strigolactone receptor D14 targets SMAX1 for degradation in response to GR24 treatment and osmotic stress. *Plant Commun*. 3: 100303.

Martinez, S.E., Conn, C.E., Guercio, A.M., Sepulveda, C., Fiscus, C.J., Koenig, D., et al. (2022) A KARRIKIN INSENSITIVE2 paralog in lettuce mediates highly sensitive germination responses to karrikinolide. *Plant Physiol*. 190: 1440–1456.

Mutuku, J.M., Cui, S., Yoshida, S. and Shirasu, K. (2021) Orobanchaceae parasite-host interactions. *New Phytol*. 230: 46–59.

Nakagawa, T., Kurose, T., Hino, T., Tanaka, K., Kawamukai, M., Niwa, Y., et al. (2007) Development of series of gateway binary vectors, pGWBs, for realizing efficient construction of fusion genes for plant transformation. *J. Biosci. Bioeng*. 104: 34–41.

Nelson, D.C.. (2021) The mechanism of host-induced germination in root parasitic plants. *Plant Physiol*. 185: 1353–1373.

Nelson, D.C., Flematti, G.R., Ghisalberti, E.L., Dixon, K.W. and Smith, S.M. (2012) Regulation of seed germination and seedling growth by chemical signals from burning vegetation. *Annu. Rev. Plant Biol*. 63: 107–130.

Nomura, S., Nakashima, H., Mizutani, M., Takikawa, H. and Sugimoto, Y. (2013) Structural requirements of strigolactones for germination induction and inhibition of Striga gesnerioides seeds. *Plant Cell Rep*. 32: 829–838.

Ogawa, S., Cui, S., White, A.R.F., Nelson, D.C., Yoshida, S. and Shirasu, K. (2022) Strigolactones are chemoattractants for host tropism in Orobanchaceae parasitic plants. *Nat. Commun*. 13: 4653.

Ogawa, S. and Shirasu, K. (2022) Strigol induces germination of the facultative parasitic plant in the absence of nitrate ions. *Plant Signal Behav*. 17: 2114647.

Seto, Y., Yasui, R., Kameoka, H., Tamiru, M., Cao, M., Terauchi, R., et al. (2019) Strigolactone perception and deactivation by a hydrolase receptor DWARF14. *Nat. Commun*. 10: 191.

Soundappan, I., Bennett, T., Morffy, N., Liang, Y., Stanga, J.P., Abbas, A., et al. (2015) SMAX1-LIKE/D53 family members enable distinct MAX2-dependent responses to strigolactones and karrikins in Arabidopsis. *Plant Cell* 27: 3143–3159.

Stanga, J.P., Morffy, N. and Nelson, D.C. (2016) Functional redundancy in the control of seedling growth by the karrikin signaling pathway. *Planta* 243: 1397–1406.

Stanga, J.P., Smith, S.M., Briggs, W.R. and Nelson, D.C. (2013) SUPPRESSOR OF MORE AXILLARY GROWTH2 1 controls seed germination and seedling development in Arabidopsis. *Plant Physiol*. 163: 318–330.

Steenwyk, J.L., Buida, T.J., 3rd, Li, Y., Shen, -X.-X., Rokas, A. and Hejnol, A. (2020) ClipKIT: a multiple sequence alignment trimming software for accurate phylogenomic inference. *PLoS Biol*. 18: e3001007.

Stirling, S.A., Guercio, A.M., Patrick, R.M., Huang, X.-Q., Bergman, M.E., Dwivedi, V., et al. (2024) Volatile communication in plants relies on a KAI2-mediated signaling pathway. *Science* 383: 1318–1325.

Stirnberg, P., Furner, I.J. and Ottoline Leyser, H.M. (2007) MAX2 participates in an SCF complex which acts locally at the node to suppress shoot branching. *Plant J*. 50: 80–94.

Sun, X.-D. and Ni, M. (2011) HYPOSENSITIVE TO LIGHT, an alpha/beta fold protein, acts downstream of ELONGATED HYPOCOTYL 5 to regulate seedling de-etiolation. *Mol. Plant* 4: 116–126.

Sun, Y.K., Yao, J., Scaffidi, A., Melville, K.T., Davies, S.F., Bond, C.S., et al. (2020) Divergent receptor proteins confer responses to different karrikins in two ephemeral weeds. *Nat. Commun*. 11: 1264.

Takei, S., Suzuki, T., Okabe, S., Nishiyama, K., Kawakami, N. and Seto, Y. (2024) Highly sensitive strigolactone perception by a divergent clade KAI2 receptor in a facultative root parasitic plant, *Phtheirospermum japonicum*. *Plant Cell Physiol*. 65: 1958–1968.

Takei, S., Uchiyama, Y., Bürger, M., Suzuki, T., Okabe, S., Chory, J., et al. (2023) A divergent clade KAI2 protein in the root parasitic plant Orobanche minor is a highly sensitive strigolactone receptor and is involved in the perception of sesquiterpene lactones. *Plant Cell Physiol*. 64: 996–1007.

Tamura, K., Stecher, G., Kumar, S. and Battistuzzi, F.U. (2021) MEGA11: molecular evolutionary genetics analysis Version 11. *Mol. Biol. Evol*. 38: 3022–3027.

Toh, S., Holbrook-Smith, D., Stogios, P.J., Onopriyenko, O., Lumba, S., Tsuchiya, Y., et al. (2015) Structure-function analysis identifies highly sensitive strigolactone receptors in Striga. *Science* 350: 203–207.

Trifinopoulos, J., Nguyen, L.-T., von Haeseler, A. and Minh, B.Q. (2016) W-IQ-TREE: a fast online phylogenetic tool for maximum likelihood analysis. *Nucleic Acids Res*. 44: W232–5.

Tsuchiya, Y., Yoshimura, M., Sato, Y., Kuwata, K., Toh, S., Holbrook-Smith, D., et al. (2015) PARASITIC PLANTS. Probing strigolactone receptors in Striga hermonthica with fluorescence. *Science* 349: 864–868.

Uraguchi, D., Kuwata, K., Hijikata, Y., Yamaguchi, R., Imaizumi, H., Am, S., et al. (2018) A femtomolar-range suicide germination stimulant for the parasitic plant Striga hermonthica. *Science* 362: 1301–1305.

Wang, L., Wang, B., Jiang, L., Liu, X., Li, X., Lu, Z., et al. (2015a) Strigolactone signaling in Arabidopsis regulates shoot development by targeting D53-Like SMXL repressor proteins for ubiquitination and degradation. *Plant Cell* 27: 3128–3142.

Wang, L., Xu, Q., Yu, H., Ma, H., Li, X., Yang, J., et al. (2020) Strigolactone and Karrikin signaling pathways elicit ubiquitination and proteolysis of SMXL2 to regulate hypocotyl elongation in Arabidopsis. *Plant Cell* 32: 2251–2270.

Wang, Y., Yao, R., Du, X., Guo, L., Chen, L., Xie, D., et al. (2021) Molecular basis for high ligand sensitivity and selectivity of strigolactone receptors in Striga. *Plant Physiol*. 185: 1411–1428.

Wang, Z.-P., Xing, H.-L., Dong, L., Zhang, H.-Y., Han, C.-Y., Wang, X.-C., et al. (2015b) Egg cell-specific promoter-controlled CRISPR/Cas9 efficiently generates homozygous mutants for multiple target genes in Arabidopsis in a single generation. *Genome Biol*. 16: 144.

Waters, M.T., Gutjahr, C., Bennett, T. and Nelson, D.C. (2017) Strigolactone signaling and evolution. *Annu. Rev. Plant Biol*. 68: 291–322.

Waters, M.T. and Nelson, D.C. (2023) Karrikin perception and signalling. *New Phytol*. 237: 1525–1541.

Waters, M.T., Nelson, D.C., Scaffidi, A., Flematti, G.R., Sun, Y.K., Dixon, K.W., et al. (2012) Specialisation within the DWARF14 protein family confers distinct responses to karrikins and strigolactones in Arabidopsis. *Development* 139: 1285–1295.

Waters, M.T., Scaffidi, A., Flematti, G. and Smith, S.M. (2015a) Substrate-induced degradation of the α/β-fold hydrolase KARRIKIN INSENSITIVE2 requires a functional catalytic triad but is independent of MAX2. *Mol. Plant* 8: 814–817.

Waters, M.T., Scaffidi, A., Moulin, S.L.Y., Sun, Y.K., Flematti, G.R. and Smith, S.M. (2015b) A Selaginella moellendorffii ortholog of KARRIKIN INSENSITIVE2 functions in Arabidopsis development but cannot mediate responses to karrikins or strigolactones. *Plant Cell* 27: 1925–1944.

White, A.R.F., Mendez, J.A., Khosla, A. and Nelson, D.C. (2022) Rapid analysis of strigolactone receptor activity in a Nicotiana benthamiana dwarf14 mutant. *Plant Direct* 6: e389.

Whitney, P.J. and Carsten, C. (1981) Chemotropic response of broomrape radicles to host root exudates. *Ann. Bot.* 48: 919–921.

Williams, C.N. (1961) Tropism and morphogenesis of Striga seedlings in the host rhizosphere. *Ann. Bot.* 25: 407–415.

Xing, H.-L., Dong, L., Wang, Z.-P., Zhang, H.-Y., Han, C.-Y., Liu, B., et al. (2014) A CRISPR/Cas9 toolkit for multiplex genome editing in plants. *BMC Plant Biol*. 14: 327.

Xu, Y., Zhang, J., Ma, C., Lei, Y., Shen, G., Jin, J., et al. (2022) Comparative genomics of orobanchaceous species with different parasitic lifestyles reveals the origin and stepwise evolution of plant parasitism. *Mol. Plant* 15: 1384–1399.

Yao, J., Mashiguchi, K., Scaffidi, A., Akatsu, T., Melville, K.T., Morita, R., et al. (2018) An allelic series at the KARRIKIN INSENSITIVE 2 locus of Arabidopsis thaliana decouples ligand hydrolysis and receptor degradation from downstream signalling. *Plant J*. 96: 75–89.

Yao, R., Ming, Z., Yan, L., Li, S., Wang, F., Ma, S., et al. (2016) DWARF14 is a non-canonical hormone receptor for strigolactone. *Nature* 536: 469–473.

Yao, R., Wang, F., Ming, Z., Du, X., Chen, L., Wang, Y., et al. (2017) ShHTL7 is a non-canonical receptor for strigolactones in root parasitic weeds. *Cell Res*. 27: 838–841.

Yoshida, S., Kim, S., Wafula, E.K., Tanskanen, J., Kim, Y.-M., Honaas, L., et al. (2019) Genome sequence of Striga asiatica provides insight into the evolution of plant parasitism. *Curr. Biol*. 29: 3041–52.e4.

Zheng, J., Hong, K., Zeng, L., Wang, L., Kang, S., Qu, M., et al. (2020) Karrikin signaling acts parallel to and additively with strigolactone signaling to regulate rice mesocotyl elongation in darkness. *Plant Cell* 32: 2780–2805.

Zhou, F., Lin, Q., Zhu, L., Ren, Y., Zhou, K., Shabek, N., et al. (2013) D14-SCF(D3)-dependent degradation of D53 regulates strigolactone signalling. *Nature* 504: 406–410.